Slowly Exchanging *cis*-PtA_2B_2 Atropisomers with A_2 = Chiral Diamine Ligands and B = 5,6-Dimethylbenzimidazole

Manuela Trani,[a] Francesco Cannito,[b] Giovanni Natile,*[c] Patricia A. Marzilli,[d] and Luigi G. Marzilli*[d]

Keywords: Cisplatin / Anticancer drug / Platinum complexes / Chiral diamines / 5,6-Dimethylbenzimidazole

cis-PtA_2G_2 complexes, in which A_2 is a bidentate amine ligand and G is a unidentate guanine derivative bound to platinum through N7, are simple models of the G-G cross-link DNA lesion formed by the anticancer drug cisplatin. Rotation of the G bases about the Pt–N7 bonds is usually rapid except for bulky amine ligand(s). This paper concerns *cis*-$PtA_2(Me_2Bzm)_2$ adducts [A_2 = 2,2′-bipiperidine (Bip) and *N*,*N*,*N*′,*N*′-tetramethyl-2,3-diaminobutane (Me_4DAB); Me_2Bzm = 5,6-dimethylbenzimidazole] for which the interconversion among possible rotamers (one HH and two HT) is slow on the NMR time scale. The amounts of the rarely observed HH conformer were 52 and 37 % at 5 °C for $BipPt(Me_2Bzm)_2$ and $Me_4DABPt(Me_2Bzm)_2$, respectively, and increased to 60 and 44 % at 50 °C. This result represents the first reported clear evidence for the existence of the HH atropisomer in *cis*-PtA_2B_2 adducts (B = G or Me_2Bzm base) with fully substituted diamines, such as Me_4DAB or Me_4EN (Me_4EN = *N*,*N*,*N*′,*N*′-tetramethyl-1,2-diaminoethane). The lack of an O-substituent on the C4 atom of Me_2Bzm (corresponding to C6 of G) undoubtedly allows for a relatively stable HH conformer. Thermodynamic parameters confirm the crucial role of the substituents in positions 4 and 6 of the base systems (for Me_2Bzm and G derivatives, respectively) in determining the stability of different rotamers. The greater abundance of the HH rotamer for $BipPt(Me_2Bzm)_2$ than for $Me_4DABPt(Me_2Bzm)_2$ indicates that an increase in the steric bulk of the carrier ligand favors the HT rotamers over the HH rotamer. For both $BipPt(Me_2Bzm)_2$ and $Me_4DABPt(Me_2Bzm)_2$ adducts, the major HT rotamer has the six-membered ring of each Me_2Bzm ligand on the more crowded side of the *cis* amine with respect to the platinum coordination plane: the N–CH_2– group in Bip and the N–Me_{eq} (N–Me_{eq} = quasi-equatorial N–Me) in Me_4DAB adducts. The latter result is in complete agreement with previous findings from our laboratories concerning $BipPtG_2$ and $Me_4DABPtG_2$ compounds and gives further support to the view that the major HT rotamer is stabilized by the six-membered ring of each base canted toward the *cis* base.

Introduction

Cisplatin [*cis*-$PtCl_2(NH_3)_2$] is one of the most widely used drugs in the treatment of several cancers.[1,2] Its precise mechanism of action is not completely understood, but it is known to target primarily nuclear DNA, forming a critical lesion by cross-linking two adjacent guanine bases or an adenine and a guanine base of the same strand.[1–6] A serious limitation in studies of adducts between Pt anticancer drugs and DNA is the fluxional character of these adducts. We have called this limitation the "dynamic motion problem."[7]

We have been investigating *cis*-PtA_2G_2 complexes, in which A_2 is a bidentate amine ligand designed to possess steric bulk near the *cis* coordination sites and G is a unidentate guanine derivative bound to platinum through N7.[7–14] In these models the interconversion between rotamers (by rotation around the Pt–N7 bonds) is slow on the NMR time scale,[15] and thus the presence of different rotamers can be detected by NMR spectroscopy. The G bases can be in a head-to-head arrangement (HH), in which both H8 atoms lie on the same side of the coordination plane, or in a head-to-tail arrangement (HT), in which the H8 atoms lie on opposite sides of the coordination plane (ΛHT and ΔHT, Scheme 1).

For $BipPtG_2$ and $Me_2DABPtG_2$ adducts (Bip = 2,2′-bipiperidine, Me_2DAB = *N*,*N*′-dimethyl-2,3-diaminobutane; C_2-symmetrical ligands are obtained for *S*,*R*,*R*,*S* or *R*,*S*,*S*,*R* configurations at the four stereocenters located on the N, C, C, and N atoms of the chelate ring, Scheme 2), the HT conformers typically dominated over the HH conformer.[11,12,16,17] This dominance was attributed to interligand interactions, which were classified as "first-to-first," "first-to-second," and "second-to-second" sphere com-

[a] Department of Chemistry, Emory University, Atlanta, GA 30322, USA
[b] Consorzio Interuniversitario di Ricerca in Chimica dei Metalli nei Sistemi Biologici (C.I.R.C.M.S.B.), Via C. Ulpiani 27, 70126 Bari, Italy
[c] Dipartimento Farmaco-Chimico, Università di Bari, Via E. Orabona 4, 70125 Bari, Italy
[d] Department of Chemistry, Louisiana State University, Baton Rouge, LA 70803, USA
E-mail: lmarzil@lsu.edu
Supporting information for this article is available on the WWW under http://www.eurjic.org or from the author.

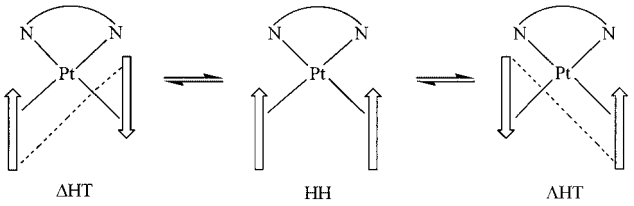

Scheme 1. Schematic representation of HH, ΔHT, and ΛHT atropisomers for *cis*-PtA_2B_2 complexes.

munications.[17,18] The latter two types of interactions involve phosphate groups,[11,12,17,18] and in this study we examine adducts lacking this group in order to focus on first-to-first sphere communications (FFC). FFC are interligand interactions involving portions of the ligands close to the metal center. Base-to-base interactions and H-bonding interactions between G O6 and N–H of a *cis* amine fall into this category. For C_2-symmetrical Bip and Me_2DAB ligands the latter interaction should favor the HT rotamer having the O6 atom of each G near the N–H of the *cis* amine, and on the opposite side of the platinum coordination plane from the N–CH_2– or the N–Me group. One HT rotamer was in fact favored but, contrary to our expectations, the O6 of each guanine of this major rotamer was near the N–CH_2– or the N–Me group of the *cis* amine, not near the N–H group.

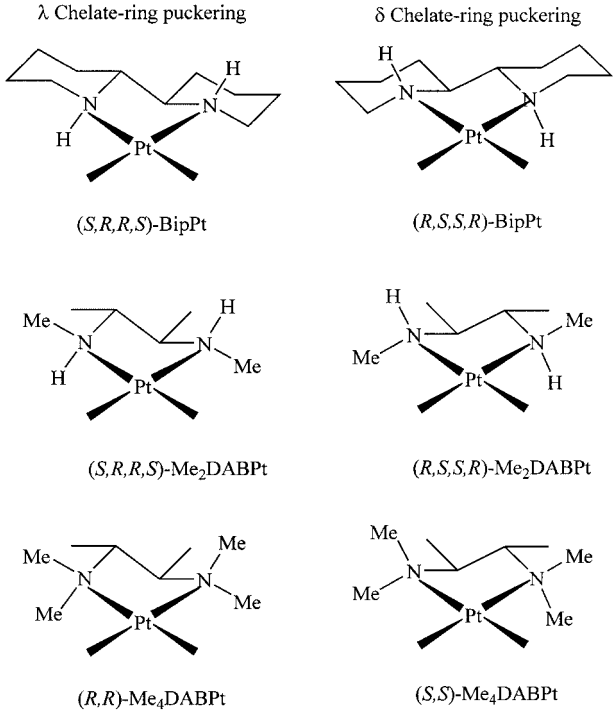

Scheme 2. Schematic representation of Bip, Me_2DAB, and Me_4DAB ligands coordinated to a platinum(II) moiety.

In the NMR spectra of $BipPtG_2$ and $Me_2DABPtG_2$ complexes, the H8 signal of the major HT rotamer is more downfield than the H8 signal of the minor HT rotamer. This result is an indication that in the major HT rotamer the H8 proton of each guanine is pointing farther away from the *cis* G (so that it experiences a smaller shielding effect from the *cis* G) as the six-membered ring of each guanine moves toward the *cis* guanine ("6-in" orientation). The HH rotamer has one H8 signal more downfield than the H8 signal of the major HT form (HH_d base), and the second H8 signal more upfield than the H8 signal of the minor HT conformer (HH_u base). The latter signal must belong to a guanine having H8 pointing toward the *cis* G and embedded in its shielding cone; therefore this guanine must have the "6-out" orientation.

The "6-in" orientation of the *cis* G's in HT conformers of $BipPtG_2$ and $Me_2DABPtG_2$ adducts has implications relevant to the stability of the conformers. For example, the interaction between the H8 atom of each G and the *cis* amine will be smaller when H8 is on the side of the N–H than when it is on the side of the N–CH_2– or the N–Me of the *cis* amine with respect to the platinum coordination plane. Therefore the conformer with H8 near the N–H of the *cis* amine will be favored and will have the six-membered ring of each guanine on the same side as the N–CH_2– or the N–Me group of the *cis* amine. The fact that the "6-in" orientation of *cis* guanines is favored suggests strongly that this orientation allows better base-base, dipole-dipole (the H8 of one guanine closer to the O6 of the second guanine), and stacking interactions.

In the HH rotamer, the "6-out" guanine (with a shielded H8) has the six-membered ring on the same side of the coordination plane as the N–H of the *cis* amine (whereas the second guanine has the six-membered ring near the N–CH_2– or the N–Me of the *cis* amine). The smaller steric interaction of the former guanine with the *cis* amine allows the "6-out" orientation to occur, and as a consequence the negatively charged O6 atom of this "6-out" guanine is farther from the O6 atom of the *cis* G.

More recently, in order to achieve a better understanding of systems lacking N–H groups, studies were conducted on adducts with the carrier ligand, Me_4DACH (Me_4DACH = *N*,*N*,*N*′,*N*′-tetramethyl-1,2-diaminocyclohexane).[19] The dissymmetry of Me_4DACH with respect to the platinum coordination plane is very small (each diamine N-donor has methyls on both sides of the coordination plane), which makes the ligand fundamentally different from the Bip and Me_2DAB ligands previously investigated. As Cramer found in his classic study on Me_4ENPtG_2 adducts (Me_4EN = *N*,*N*,*N*′,*N*′-tetramethyl-1,2-diaminoethane, G = Guo),[15] no HH rotamer was observed at equilibrium in any of the $Me_4DACHPtG_2$ adducts; moreover, the H8 chemical shifts are very similar for the major and the minor HT rotamers. The absence of a significant amount of HH rotamer could be a consequence of the bulk produced on both sides of the coordination plane by the four N–Me groups. This bulk on both sides of the coordination plane does not allow "6-out" canting of at least one G, which is required for minimizing O6···O6 electrostatic repulsions.[20] Moreover, two $Me_4DACHPt(5'\text{-}GMP)_2$ ΔHT rotamers were shown by X-ray crystallography to have a "6-in" orientation of the two G's in spite of the opposite chiralities of the Me_4DACH ligands in the two compounds.[21]

Despite the many studies conducted on cisplatin models, numerous questions remain unanswered. In an effort to achieve a better understanding of the factors influencing formation and stability of conformers in models of the cisplatin-DNA cross-link, we undertook a study of *cis*-PtA_2-$(Me_2Bzm)_2$ complexes (A_2 = Bip and Me_4DAB; Me_2Bzm = 5,6-dimethylbenzimidazole; Scheme 3). Me_2Bzm lacks the O substituent on the C4 atom (corresponding to C6 of purines); therefore, a comparison between Me_2Bzm and G adducts allows us to unravel the role of such an oxygen atom in the formation and stability of conformers. Moreover, Me_2Bzm has several "probe protons" on its periphery that might help in assessing the ligand canting.[22]

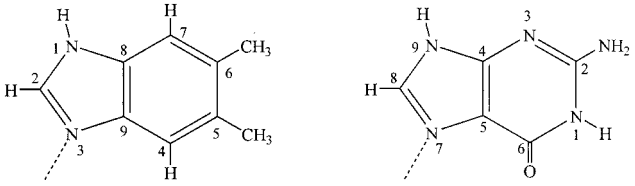

Scheme 3. Shorthand drawings of 5,6-dimethylbenzimidazole and guanine bases.

Results

[*rac*-BipPt($Me_2Bzm)_2$]$^{2+}$ Complex: The lack of chirality in the Me_2Bzm ligands renders indistinguishable the NMR spectroscopic data obtainable for [*rac*-BipPt-$(Me_2Bzm)_2]^{2+}$ and for the single enantiomers [(*R*,*S*,*S*,*R*)-BipPt$(Me_2Bzm)_2]^{2+}$ and [(*S*,*R*,*R*,*S*)-BipPt$(Me_2Bzm)_2]^{2+}$; therefore, only the NMR spectroscopic data concerning the *rac* isomer (used in higher concentration) will be described. The ^{1}H NMR spectrum of [*rac*-BipPt$(Me_2Bzm)_2]^{2+}$ (in D_2O at pH 6 and 5 °C) exhibited four sets of signals for each proton (Figure 1 shows the H2 region), indicating the presence of one HH and two HT conformers. Complete assignment of the signals for each conformer (Table 1) was possible on the basis of a ^{1}H/^{1}H ROESY experiment carried out at 5 °C. In the ^{1}H/^{1}H ROESY spectrum, the H2 signal at δ = 8.57 ppm had an NOE cross-peak to the H2 signal at δ = 8.42 ppm, allowing the assignment of these signals to the HH conformer (HH_d and HH_u denote the HH base having the H2 signal downfield and upfield with respect to the H2 signal of the major HT rotamer, respectively). The other two signals at δ = 8.54 and 8.38 ppm must belong to the major HT (MHT) and minor HT (mHT) rotamers, respectively. The H2 signal of the major HT conformer at δ = 8.54 ppm had an NOE cross-peak to the H4 signal at δ = 8.16 ppm; similarly, the H2 signal of the minor HT conformer at δ = 8.38 ppm had an NOE cross-peak to the H4 signal at δ = 8.18 ppm. Therefore, the H4 signals at δ = 8.16 and 8.18 ppm were assigned to the major and minor HT conformers, respectively. The remaining two H4 signals belonging to the HH rotamer (8.08 and 8.29 ppm) were assigned to the HH_d and HH_u bases of the HH rotamer, respectively, on the basis of the opposite relationship in chemical shift between the H2 and H4 protons.

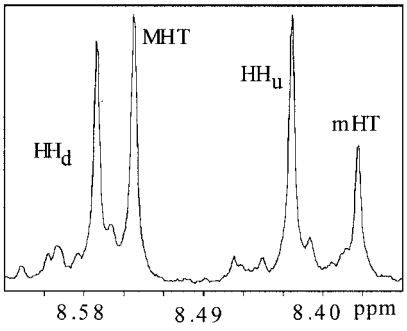

Figure 1. H2 region of the ^{1}H NMR spectrum of [*rac*-BipPt$(Me_2Bzm)_2]^{2+}$ at 5 °C.

Table 1. ^{1}H NMR Shifts (ppm) of Me_2Bzm for [*rac*-BipPt$(Me_2Bzm)_2]^{2+}$ at 5 °C and pH 6.

	MHT[a]	mHT[a]	HH_d[a]	HH_u[a]
H2	8.54	8.38	8.57	8.42
H4	8.16	8.18	8.08	8.29
H7	7.29	7.37	7.21	7.26
Me5	2.42	2.49	2.21	2.47
Me6	2.24	2.34	2.01	2.20

[a] MHT = equivalent bases of the major head-to-tail conformer; mHT = equivalent bases of the minor head-to-tail conformer; HH_d = base of the HH conformer with downfield H2; HH_u = base of the HH conformer with upfield H2.

NOE cross-peaks between H4 and Me5 signals, between Me5 and Me6 signals, and between Me6 and H7 signals were used to complete the assignments of the Me_2Bzm protons (Supporting information; for supporting information see also the footnote on the first page of this article). NOE cross-peaks between the H4 signals of Me_2Bzm and the N–CH_2– signals of Bip allowed us to assign the Δ or Λ conformations to the HT rotamers and to identify the orientation of each base in the HH rotamer. The H4 signal at δ = 8.16 ppm belonging to the major HT conformer had a cross-peak to the N–CH_2– signal of the Bip ligand at δ = 2.78 ppm. Therefore, the major HT rotamer has the Me_2Bzm six-membered rings close to the *cis* N–CH_2– groups of the Bip ligand [this corresponds to the rotamer having the ΔHT conformation in the (*R*,*S*,*S*,*R*) adduct and the ΛHT conformation in the (*S*,*R*,*R*,*S*) adduct]. It follows that the minor HT rotamer must have the six-membered ring of each Me_2Bzm near the N–H of the *cis* amine corresponding to ΛHT and ΔHT conformations for the (*R*,*S*,*S*,*R*) and (*S*,*R*,*R*,*S*) adducts, respectively. The H4 signal at δ = 8.08 ppm belonging to the HH_d base of the HH conformer also had a cross-peak to the N–CH_2– signals of the Bip ligand at δ = 2.78 ppm, therefore the HH_d base of the HH rotamer has the six-membered ring near the *cis* N–CH_2– group of Bip. Thus, the HH_u base of the HH rotamer must have the six-membered ring close to the N–H of the *cis* amine.

When the temperature was increased from 5 to 50 °C, a change in the ratio of conformers was observed and the HH conformer became more favored. The respective percentages of HH, major HT, and minor HT conformers were 52, 31, and 17, at 5 °C; 57, 30, and 13, at 35 °C; and 60, 28, and 12, at 50 °C.

[(*R*,*S*,*S*,*R*)-BipPt(Me_2Bzm)$_2$]$^{2+}$ and [(*S*,*R*,*R*,*S*)-BipPt(Me_2Bzm)$_2$]$^{2+}$ Complexes: The reason for preparing derivatives with pure enantiomeric Bip ligands was to investigate their CD spectra. The CD spectrum at pH 6 of [(*R*,*S*,*S*,*R*)-BipPt(Me_2Bzm)$_2$]$^{2+}$ exhibits positive bands around 300 and 260 nm and negative bands around 285, 240, and 210 nm. On the other hand, the CD spectrum at pH 6 of [(*S*,*R*,*R*,*S*)-BipPt(Me_2Bzm)$_2$]$^{2+}$ shows negative bands at 300 and 260 nm and positive bands at 285, 240, and 210 nm (Figure 2). The CD spectra of *cis*-Pt(Me_2Bzm)$_2$ adducts are not expected to be similar to those of *cis*-PtG_2 adducts because of the different nature of the $\pi \rightarrow \pi^*$ electron transitions; however, the trends observed for chiral BipPt(Me_2Bzm)$_2$ adducts at long wavelengths (>230 nm) resemble the trends observed for $BipPtG_2$ adducts. For instance, the CD spectrum of (*R*,*S*,*S*,*R*)-BipPt(5′-GMP)$_2$ at neutral pH exhibits a negative band at 288 nm and a positive band at 254 nm (which were identified as characteristic of a ΔHT conformation); conversely, the CD spectrum of (*S*,*R*,*R*,*S*)-BipPt(5′-GMP)$_2$ exhibits a positive band at 288 nm and a negative band at 254 nm (which were identified as characteristic of a ΛHT conformation).[12] Therefore, the CD spectra are in agreement with a dominant ΔHT rotamer for [(*R*,*S*,*S*,*R*)-BipPt(Me_2Bzm)$_2$]$^{2+}$ and a dominant ΛHT rotamer for [(*S*,*R*,*R*,*S*)-BipPt(Me_2Bzm)$_2$]$^{2+}$. This result is in full agreement with the NMR investigation showing that the major rotamer had the ΔHT conformation for [(*R*,*S*,*S*,*R*)-BipPt(Me_2Bzm)$_2$]$^{2+}$ and the ΛHT conformation for [(*S*,*R*,*R*,*S*)-BipPt(Me_2Bzm)$_2$]$^{2+}$.

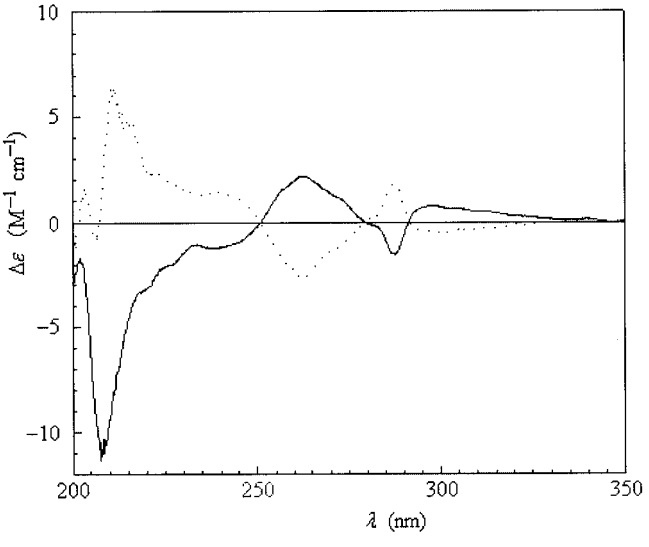

Figure 2. CD spectra of [(*R*,*S*,*S*,*R*)-BipPt(Me_2Bzm)$_2$]$^{2+}$ (solid line) and [(*S*,*R*,*R*,*S*)-BipPt(Me_2Bzm)$_2$]$^{2+}$ (dotted line) collected at room temperature and pH 6.

[*rac*-Me_4DABPt(Me_2Bzm)$_2$]$^{2+}$ Complex: As for the Bip complexes, the lack of chirality in the Me_2Bzm ligand renders the NMR spectroscopic data obtained for [*rac*-Me_4DABPt(Me_2Bzm)$_2$]$^{2+}$ identical to those obtained for complexes with individual Me_4DAB enantiomers. Therefore, only the NMR spectroscopic data concerning the *rac* isomer (used in higher concentration) will be described. The ^{1}H NMR spectrum of [*rac*-Me_4DABPt(Me_2Bzm)$_2$]$^{2+}$ (D_2O, pH 6.5, 5 and 25 °C) had four sets of signals, indicating the presence of one HH (with inequivalent bases) and two HT conformers (each one with equivalent bases) as expected (Figure 3). Complete assignment of signals for each conformer (Table 2 and Table 3) was possible on the basis of ^{1}H/^{1}H NOESY and ^{1}H/^{13}C HMQC experiments, and on the basis of previous results from these laboratories on the (*S*,*S*)-Me_4DABPt(3′-GMP)$_2$ adduct.[23]

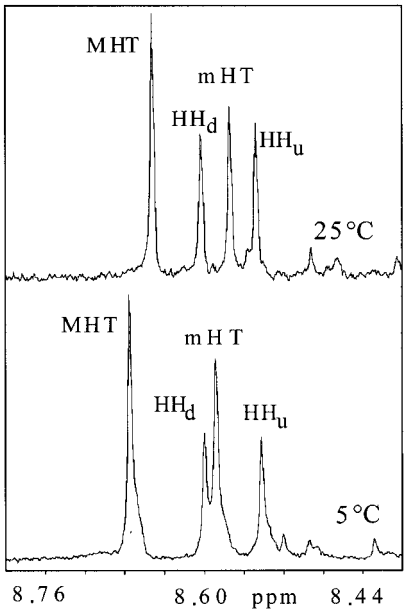

Figure 3. H2 region of the ^{1}H NMR spectra of [*rac*-Me_4DABPt(Me_2Bzm)$_2$]$^{2+}$ at 5 (bottom) and 25 °C (top).

In the ^{1}H/^{1}H NOESY spectrum of [*rac*-Me_4DABPt(Me_2Bzm)$_2$]$^{2+}$ at 5 °C, the intense H2 signal at δ = 8.67 ppm had a cross-peak to the intense H4 signal at δ = 8.17 ppm; thus, these resonances were assigned to the major HT rotamer. The less intense H2 signal at δ = 8.59 ppm had a cross-peak to the less intense H4 signal at δ = 8.19 ppm; thus, these resonances were assigned to the minor HT rotamer. The two H2 signals of equal intensity at δ = 8.60 and 8.54 ppm must belong to the HH rotamer (HH_d and HH_u bases, respectively). The H4 signals at δ = 8.27 and 8.28 ppm must also belong to the HH rotamer. Their assignment to the HH_u and HH_d bases, respectively, was possible on the basis of NOE cross-peaks between the H4 protons and the *cis* amine N–Me's as described in the following paragraph. NOE cross-peaks be-

Table 2. ^{1}H NMR Shifts (ppm) of Me_2Bzm and Amine N–Me's for [*rac*-$Me_4DABPt(Me_2Bzm)_2]^{2+}$ at 5 and 25 °C and at pH 6.

	5 °C				25 °C			
	MHT[a]	mHT[a]	HH_d[a]	HH_u[a]	MHT	mHT	HH_d	HH_u
H2	8.67[b]	8.59[c]	8.60[b]	8.54[c]	8.65	8.57	8.60	8.54
H4	8.17[c]	8.19[b]	8.28[c]	8.27[b]	8.17	8.19	8.27	8.25
H7	7.25	7.26	7.15	7.16	7.31	7.32	7.23	7.24
Me5	2.41	2.42	2.33	2.37	2.45	2.46	2.41	2.43
Me6	2.22	2.24	2.06	2.09	2.30	2.31	2.20	2.21
N–Me(ax)	2.89	2.73	2.79	2.85	2.91	2.75	2.81	2.88
N–Me(eq.)	2.58	2.78	2.69	2.65	2.60	2.79	2.71	2.67

[a] MHT = equivalent bases of major head-to-tail conformer; mHT = equivalent bases of minor head-to-tail conformer; HH_d = base of the HH conformer with downfield H2; HH_u = base of the HH conformer with upfield H2. [b] Near "quasi-axial" N–Me. [c] Near "quasi-equatorial" N–Me.

Table 3. ^{13}C NMR Shifts (ppm) of Me_2Bzm and Amine N–Me's for [*rac*-$Me_4DABPt(Me_2Bzm)_2]^{2+}$ at 25 °C and pH 6.

	MHT[a]	mHT[a]	HH_d[a]	HH_u[a]
C2	145.0	145.4	144.8	145.0
C4	119.6	119.5	120.8	120.5
C7	116.3	116.3	116.1	116.1
Me5	22.5	22.6	22.5	22.5
Me6	22.4	22.4	22.3	22.3
N–Me(ax)	45.2	47.0	46.3	47.2
N–Me(eq.)[b]	53.6 (14.6)	52.6 (18.2)	53.9 (13.4)	52.8 (18.2)

[a] MHT = equivalent bases of the major head-to-tail conformer; mHT = equivalent bases of the minor head-to-tail conformer; HH_d = base of the HH conformer with downfield H2; HH_u = base of the HH conformer with upfield H2. [b] $^3J(^1H,^{13}C)$ in Hz, given in parentheses.

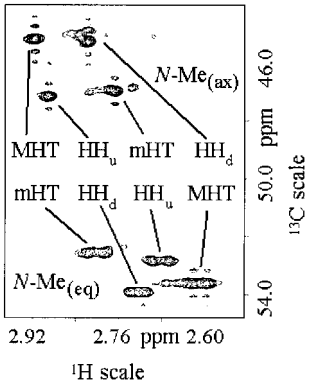

Figure 4. N–Me region of the ^{1}H/^{13}C HMQC spectrum (25 °C) of [*rac*-$Me_4DABPt(Me_2Bzm)_2]^{2+}$.

tween H4 and Me5 signals, between Me5 and Me6 signals, and between Me6 and H7 signals were used to complete the assignments of the Me_2Bzm signals (Supporting Information).

Assignment of the Δ and Λ conformations to the two HT rotamers and of the HH_d and HH_u bases in the HH rotamer was derived from the relative positions of the H2 (five-membered ring) and H4 (six-membered ring) protons with respect to the N–Me_{ax} and N–Me_{eq} (quasi-axial and quasi-equatorial N–Me groups of the carrier ligand, respectively) as revealed by the ^{1}H/^{1}H NOESY spectrum.[24] The latter experiment depends on the assignment of the proton resonances to the axial and equatorial N–Me's of the Me_4DAB ligand. This assignment was made on the basis of a previous investigation carried out in these laboratories on the (*S*,*S*)-$Me_4DABPt(3'\text{-GMP})_2$ adduct,[23] showing that the equatorial N–Me resonances have ^{13}C NMR chemical shifts at ca. 53 ppm, while the axial N–Me resonances have ^{13}C NMR chemical shifts at ca. 46 ppm. Therefore the ^{1}H/^{13}C HMQC experiment reported in Figure 4 was sufficient to distinguish between axial and equatorial N–Me signals.

The strong NOE cross-peaks observed between the H2 and the N–Me_{ax} signals and between the H4 and the N–Me_{eq} signals for the major HT conformer provide evidence that the six-membered ring of each base is near the N–Me_{eq} group of the *cis* amine; thus, the MHT rotamer has the ΔHT conformation for the [(*S*,*S*)-$Me_4DABPt(Me_2Bzm)_2]^{2+}$ adduct and the ΛHT conformation for the [(*R*,*R*)-$Me_4DABPt(Me_2Bzm)_2]^{2+}$ adduct. Likewise, strong NOE cross-peaks between the H2 and the N–Me_{eq} signals and between the H4 and the N–Me_{ax} signals for the minor HT conformer are indications that the six-membered ring is close to the N–Me_{ax} group of the *cis* amine, a situation which corresponds to the mHT atropisomer having the ΛHT conformation in the [(*S*,*S*)-$Me_4DABPt(Me_2Bzm)_2]^{2+}$ adduct and the ΔHT conformation in the [(*R*,*R*)-$Me_4DABPt(Me_2Bzm)_2]^{2+}$ adduct. For the HH rotamer, a strong NOE cross-peak between H2 and N–Me_{ax} signals for the HH_d base indicates that this base has the six-membered ring near the N–Me_{eq} of the *cis* amine. The H4 signal at δ = 8.28 ppm has a NOE cross-peak to an equatorial N–Me signal (δ = 2.69 ppm); thus, it is assigned to the HH_d base. On the other hand, a strong NOE cross-peak between the H2 and the N–Me_{eq} signals for the HH_u base indicates that this base has the six-membered ring close to the N–Me_{ax} of the *cis* amine. The H4 signal at δ = 8.27 ppm has a NOE cross-peak to an axial N–Me signal (δ = 2.85 ppm); thus, it is assigned to the HH_u base. The H2/N–Me and H4/N–Me regions of ^{1}H/^{1}H NOESY spectra for [*rac*-$Me_4DABPt(Me_2Bzm)_2]^{2+}$ are reported in Figure 5 and Figure 6, respectively.

As found also for the [*rac*-$BipPt(Me_2Bzm)_2]^{2+}$ adduct, the percentages of the different [*rac*-$Me_4DABPt(Me_2Bzm)_2]^{2+}$ conformers depend on temperature. The relative abundances of the HH, major HT, and minor HT conformers were 37, 39, and 24, at 5 °C; 42, 35, and 23, at 25 °C; and 44, 35, and 21, at 50 °C.

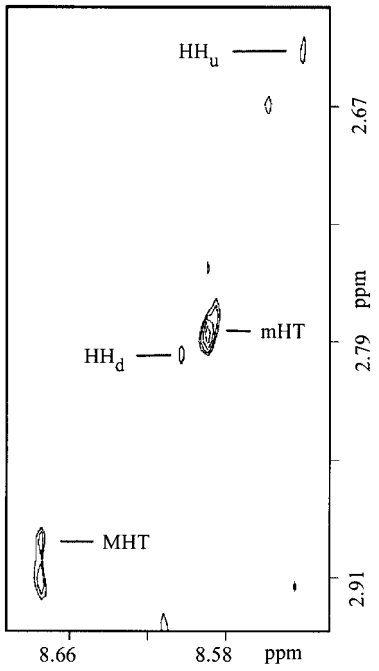

Figure 5. H2/NMe region of the $^1H/^1H$ NOESY spectrum of [*rac*-$Me_4DABPt(Me_2Bzm)_2]^{2+}$ at 5 °C.

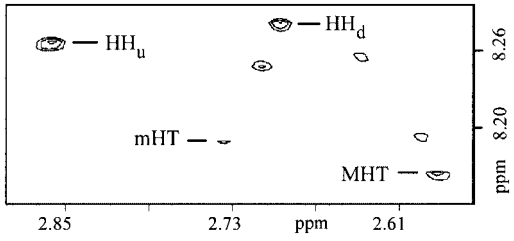

Figure 6. H4/N–Me region of the $^1H/^1H$ NOESY spectrum of [*rac*-$Me_4DABPt(Me_2Bzm)_2]^{2+}$ at 5 °C.

[(*S*,*S*)-$Me_4DABPt(Me_2Bzm)_2]^{2+}$ and [(*R*,*R*)-$Me_4DABPt(Me_2Bzm)_2]^{2+}$ Complexes: CD data for both [(*S*,*S*)-$Me_4DABPt(Me_2Bzm)_2]^{2+}$ and [(*R*,*R*)-$Me_4DABPt(Me_2Bzm)_2]^{2+}$ adducts have been collected. The CD spectrum at pH 6 of [(*S*,*S*)-$Me_4DABPt(Me_2Bzm)_2]^{2+}$ exhibits positive bands around 300, 275, and 210 nm, and a negative band at 240 nm. In contrast, the CD spectrum at pH 6 of [(*R*,*R*)-$Me_4DABPt(Me_2Bzm)_2]^{2+}$ shows negative bands at 300, 275, and 210 nm, and a positive band at 240 nm (Figure 7). Thus, the CD spectra of [(*S*,*S*)-$Me_4DABPt(Me_2Bzm)_2]^{2+}$ and [(*R*,*R*)-$Me_4DABPt(Me_2Bzm)_2]^{2+}$ resemble those observed for [(*R*,*S*,*S*,*R*)-$BipPt(Me_2Bzm)_2]^{2+}$ and [(*S*,*R*,*R*,*S*)-$BipPt(Me_2Bzm)_2]^{2+}$ only for wavelengths above 230 nm, while they are rather different for wavelengths below 230 nm. Moreover, for wavelengths above 230 nm the Cotton effect is dominated by coupling between $\pi \rightarrow \pi^*$ transitions of *cis* bases and can be diagnostic for the Λ or Δ conformation of the dominant HT rotamer.[21] Thus for the Me_4DAB complexes also, as previously observed for the Bip adducts, the CD spectra are in agreement with the dominance of the ΔHT conformation for [(*S*,*S*)-$Me_4DABPt(Me_2Bzm)_2]^{2+}$ and of the ΛHT conformation for [(*R*,*R*)-$Me_4DABPt(Me_2Bzm)_2]^{2+}$. This result is in full agreement with the NMR spectroscopic data showing that the major HT rotamer had the Δ conformation in the [(*S*,*S*)-$Me_4DABPt(Me_2Bzm)_2]^{2+}$ adduct and the Λ conformation in the [(*R*,*R*)-$Me_4DABPt(Me_2Bzm)_2]^{2+}$ adduct.

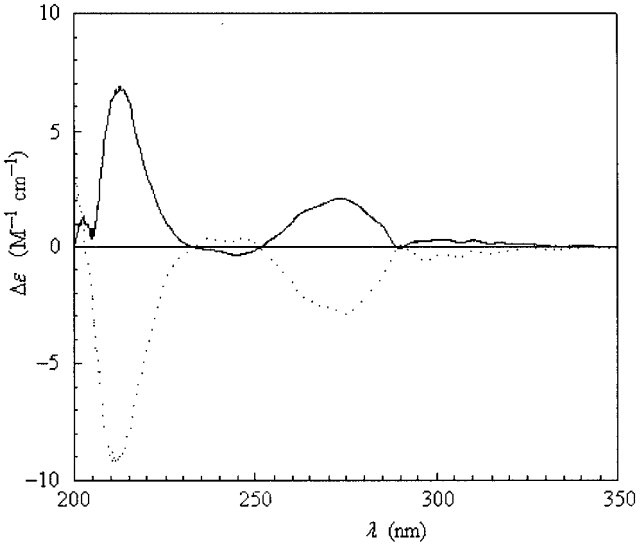

Figure 7. CD spectra of [(*S*,*S*)-$Me_4DABPt(Me_2Bzm)_2]^{2+}$ (solid line) and [(*R*,*R*)-$Me_4DABPt(Me_2Bzm)_2]^{2+}$ (dotted line) collected at room temperature and pH 6.

From the percentages of individual rotamers at different temperatures the activation parameters for the equilibria HH ⇄ MHT and HH ⇄ mHT have been evaluated and the values are reported in Table 4.

Table 4. Enthalpy (ΔH, kJ·mol^{-1}) and Entropy (ΔS, J K^{-1} mol^{-1}) for the Equilibria HH ⇄ MHT and HH ⇄ mHT (K_{MHT} = [MHT]/[HH]; K_{mHT} = [mHT]/[HH]) in *cis*-PtA_2B_2 Complexes.[a]

		ΔH	ΔS
[*rac*-$BipPt(Me_2Bzm)_2]^{2+}$	MHT	–3.9 (0.9)	–18.1 (2.8)
	mHT	–8.2 (0.3)	–38.9 (1.0)
[*rac*-$Me_4DABPt(Me_2Bzm)_2]^{2+}$	MHT	–4.6 (1.9)	–16.5 (6.4)
	mHT	–5.1 (0.4)	–21.9 (1.4)

[a] Figures in parentheses are the root mean square errors.

Discussion

Base Canting in *cis*-PtA_2B_2 Adducts: The G H8 signals are generally used as a probe for assessing the degree and direction ("6-in" or "6-out") of base canting in *cis*-PtA_2G_2 adducts.[25] In the HH conformer of $BipPtG_2$ and $Me_2DABPtG_2$ adducts (with C_2-symmetry of the bidentate ligand), one base generally has low canting, while the other base is strongly canted. For the highly canted base, the six-membered ring moves toward the *cis* amine, and the H8 atom moves toward the *cis* G. Because of the ring-current anisotropy of the *cis* G, the H8 signal of the canted G experiences an upfield shift. The H2 of Me_2Bzm is in a position corresponding to that of H8 of a G base; therefore, the canting can be deduced from the position of the H2 ^1H

NMR resonance of [*cis*-$PtA_2(Me_2Bzm)]^{2+}$ adducts. Moreover, for the Me_2Bzm ligand, the H4 and Me5 shifts can also be used to confirm the direction and degree of canting.

Of particular significance is the very small difference in H2 chemical shifts of the HH rotamer of [BipPt-$(Me_2Bzm)_2]^{2+}$ (δ = 0.15 ppm) when compared to that of the H8 signals of the HH rotamer of $BipPtG_2$ species (ca. 1.3 ppm). For *cis*-PtG_2 adducts unfavorable electrostatic and steric interactions between O6 atoms of *cis* G's are likely in the HH rotamer, for which the O6···O6 distance can be estimated to be smaller than the sum of the van der Waals radii for guanines orthogonal to the platinum coordination plane.[26] Some relief from unfavorable electrostatic and steric interactions can be achieved if one or both G's can be canted "6-out". Such a canting is possible in $BipPtG_2$ as well as in $Me_2DABPtG_2$ adducts because one G in the HH rotamer has the six-membered ring adjacent to the N–H of the *cis* amine. The "6-out" canting of this guanine will not only be allowed by the small steric interaction between the six-membered ring of the guanine and the N–H of the *cis* amine, but might also be favored by H-bond formation between the G-O6 and the amine N–H.

The main difference between G and Me_2Bzm bases resides in the absence, in the latter case, of the oxygen substituent. The absence of such a substituent greatly reduces the steric and electrostatic interactions between *cis*-bases, which therefore can both be "quasi orthogonal" to the coordination plane.

For $BipPtG_2$ adducts,[12] the H8 signal of the major HT conformer was 0.3 to 0.5 ppm downfield from the H8 signal of the minor HT conformer (depending upon the G base and the pH); in contrast, in $[BipPt(Me_2Bzm)_2]^{2+}$ the difference in chemical shift between the H2 signals of the major and minor HT rotamers is only 0.16 ppm. For HT conformers of *cis*-PtG_2 adducts base canting is driven by dipole-dipole interactions. Calculations show that a "6-in" canting of the two guanines (up to 20° rotation about the Pt–N7 bond, starting from the plane of each guanine orthogonal to the coordination plane) will bring the H8 of each guanine closer to the O6 of the *cis* guanine with consequent increase in stability of the rotamer.[28] This situation is probably attained in the MHT rotamer of $BipPtG_2$ and $Me_2DABPtG_2$ compounds, in which the H8 atom of each guanine is on the same side as the N–H of the *cis* amine with respect to the coordination plane. In contrast, in the minor HT rotamer of $BipPtG_2$ and $Me_2DABPtG_2$ compounds such a "6-in" canting of the two guanines is limited by steric interaction between the H8 of each guanine and the *N*-alkyl substituent on the *cis* amine, both on the same side of the coordination plane. With respect to the MHT rotamer, the smaller "6-in" canting of the two guanines in mHT causes both a lower stability of this rotamer and a greater shielding of the H8 protons, which therefore resonate at higher field.

In the Me_2Bzm adducts there is no strong dipole-dipole interaction of the type just described for the G adducts. Any dipole-dipole interaction should be weak. The absence of a strong driving force to base canting explains why the separation between the H2 resonances of HT rotamers is smaller in Me_2Bzm adducts than in G adducts.

As mentioned, information about canting can also be gained from the H4 and Me5 signals of Me_2Bzm. The H4 and Me5 signals of the major HT rotamer were slightly upfield with respect to the corresponding signals for the minor HT rotamer ($\Delta\delta$ of 0.02 and 0.07 ppm for H4 and Me5, respectively). The differences in chemical shift between the two H4 and between the two Me5 signals of the HH rotamer were 0.21 and 0.26 ppm, respectively (Table 1). As expected, the trend in chemical shifts for H4 and Me5 is opposite to that for H2 because canting that brings H2 closer to the *cis* base will bring H4 and Me5 farther from the *cis* base and vice-versa.

As observed in the case of $[BipPt(Me_2Bzm)_2]^{2+}$, for $[Me_4DABPt(Me_2Bzm)_2]^{2+}$ the separations between the two H2 signals of the HH rotamer (δ = 0.06 ppm) and between the H2 signals of the two HT conformers (δ = 0.08 ppm) are also small (Table 2). The explanation given for the former complex applies also to the latter.

The slightly greater separation between the two H2 resonances of the HH rotamer and between the H2 resonances of the two HT rotamers for the $[BipPt(Me_2Bzm)_2]^{2+}$ vs. the $[Me_4DABPt(Me_2Bzm)_2]^{2+}$ adduct is in agreement with the former complex having a greater canting freedom for one Me_2Bzm ligand of the HH rotamer (the Me_2Bzm having the six-membered ring adjacent to the N–H of the *cis* amine) and for the two Me_2Bzm ligands of one HT rotamer (the rotamer having the H2 of each Me_2Bzm near the N–H of the *cis* amine). However, as already pointed out, the degree of canting observed in the $[BipPt(Me_2Bzm)_2]^{2+}$ adduct is far smaller than that observed in the $BipPtG_2$ adducts because in the latter case the steric and electrostatic repulsion between the O6's of the *cis* G's in the HH conformer or the electrostatic attraction between the O6 of one G and the H8 of the *cis* G in the HT rotamers drives the tilting of the guanine(s).

Comparison with Base Canting in Re or Ru Metal Complexes Containing *cis*-Benzimidazole Ligands: The current work complements our previous studies on Re and Ru complexes containing *cis* Me_3Bzm (Me_3Bzm = 1,5,6-trimethylbenzimidazole) ligands.[22,27] For $[Re_2O_3Cl_4(Me_3Bzm)_4]$,[27] the four Me_3Bzm ligands have an HH-HT-HH arrangement. The central HT arrangement was formed by pseudo-bridging "stacked" Me_3Bzm ligands (designated as Me_3Bzm^s), while the peripheral HH arrangements were formed by one Me_3Bzm^s base and one of the two equivalent "terminal" Me_3Bzm bases (designated as Me_3Bzm^t). The structure showed that the two Me_3Bzm^t bases were highly canted with respect to the two Me_3Bzm^s bases. In the ^1H NMR spectrum the H2 signal of the Me_3Bzm^t bases was ≈ 1.3 ppm downfield from that of the Me_3Bzm^s H2 signal; the H4 and Me5 signals showed the opposite trend. The high degree of canting of the Me_3Bzm^t bases with respect to the Me_3Bzm^s bases was attributed to the electrostatic attraction between the positively charged H2 of Me_3Bzm^t and the negatively charged O and Cl groups in the core of the dimer.

For *cis*,*cis*,*cis*-[$RuCl_2(Me_2SO)_2(Me_3Bzm)_2$] ($Me_2SO$ = dimethyl sulfoxide)[22] one HT and one HH form were observed in solution. For the HH conformer, the H2 signal of the uncanted Me_3Bzm base that is *cis* to the Cl atoms was 1.5 ppm downfield with respect to the H2 signal of the canted Me_3Bzm base that is *cis* to the Me_2SO groups. Opposite trends were observed for the H4 and Me5 signals. In the X-ray structure of the HH conformer, the Me_3Bzm close to the Me_2SO groups was highly canted, with the H2 atom pointing toward the Me_3Bzm base close to the Cl atoms. The six-membered ring of the canted Me_3Bzm ligand was inserted between the two *cis* Me_2SO ligands so as to avoid steric interaction with the bulky Me_2SO groups. This insertion causes the H2 atom to move toward the *cis* Me_3Bzm. The latter Me_3Bzm is kept in a fixed position because of favorable electrostatic attraction between its H2 and the two *cis* Cl ligands.

The results obtained with the Re and Ru complexes emphasize the role of electrostatic interactions in determining the canting of Me_2Bzm/Me_3Bzm ligands. Electrostatic interactions of this type are not present in the platinum complexes investigated here, which, in fact, show little or negligible canting.

Distribution of Conformers: The HH rotamer, disfavored in most of the previously studied *cis*-PtG_2 adducts,[17] is the most favored conformer for [$BipPt(Me_2Bzm)_2$]$^{2+}$ and [$Me_4DABPt(Me_2Bzm)_2$]$^{2+}$ complexes, and its stability increases with increasing temperature. The HH:HT ratio was 1.1 at 5 °C and 1.5 at 50 °C for [$BipPt(Me_2Bzm)_2$]$^{2+}$, whereas the maximum observed HH:HT ratio was 0.8 for $BipPt(1\text{-Me-}5'\text{-GMP})_2$ complexes and was generally less than 0.3 for N1 unmethylated guanine adducts.[17]

Dipole–dipole interactions appear to play a crucial role in determining the stability of the HT rotamers in G complexes. Such interactions favor the HT rotamers over the HH rotamer because in the former case the positive end of one dipole (near the H8 atom) can approach the negative end of the second dipole (near the O6 atom). Moreover, the H8 and O6 atoms of *cis* guanines can approach each other more closely if each guanine is canted "6-in". The HH rotamer is formed in small yield in $BipPtG_2$ and $Me_2DABPtG_2$ complexes and is practically absent in the $Me_4DACHPtG_2$ adducts. In the former cases, one G (that having the six-membered ring adjacent the N–H of the *cis* amine) can be canted "6-out" so as to bring the O6 atom of one G farther from the O6 atom of the *cis* G. Such a "6-out" canting is not possible in the $Me_4DACHPtG_2$ complex because of steric interaction between the six-membered ring of each guanine and the adjacent Me-substituent on the *cis* amine; therefore, no HH rotamer is formed.

The absence of dipole-dipole interaction in Me_2Bzm adducts makes the HH and the two HT rotamers comparable in stability, with the consequence that the three rotamers are found in comparable amounts.

The slightly greater percentage of the HH rotamer for [$BipPt(Me_2Bzm)_2$]$^{2+}$ than for [$Me_4DABPt(Me_2Bzm)_2$]$^{2+}$ can be explained by the presence in the former case of a smaller steric interaction between the two six-membered rings of the Me_2Bzm ligands: for the HH rotamer these rings are on the same side of the coordination plane. In fact, in the Bip complex one Me_2Bzm has the six-membered ring on the same side of the plane as the N–H of the *cis* amine and thus the Me_2Bzm can be canted "6-out"; in contrast, in the Me_4DAB complex, both Me_2Bzm ligands have the six-membered ring on the side of one N–Me of the *cis* amine, a situation which greatly reduces the possibility of canting. However, even in the Me_4DAB complex, one Me_2Bzm (the one having the six-membered ring on the side of the plane as the "quasi axial" N–Me of the *cis* amine) can be canted "6-out" slightly more than the other Me_2Bzm (the one having the six-membered ring on the same side of the plane as the "quasi equatorial" N–Me). As a consequence, the H2 proton of the former base is more shielded by the *cis* base and resonates at higher field (HH_u) than the other (HH_d).

In both the Bip and Me_4DAB complexes with two *cis* G's or two *cis* Me_2Bzm ligands, one HT rotamer is more abundant than the other. Moreover, the major HT rotamer has the H8 or H2 signals (for G and Me_2Bzm adducts, respectively) downfield from that of the minor HT rotamer, an indication that these protons are less shielded by the *cis* base in the major HT rotamer than in the minor HT rotamer and that the two bases are more canted "6-in" in MHT than in mHT. Why the Me_2Bzm bases tend to be canted "6-in" in the HT rotamers is not clear. One possibility is that a stacking interaction can take place between *cis* Me_2Bzm bases. Therefore, as in the case of *cis* guanines, a "6-in" canting of the two bases is preferred because it ensures better stacking. Moreover, the canting can be greater when H2 is adjacent to the N–H (Bip complex) or to the "quasi axial" N–Me (Me_4DAB complex) of the *cis* amine than when H2 is adjacent to the N–CH_2– or to the "quasi equatorial" N–Me of the *cis* amine.

Thermodynamic Parameters: Both the MHT and mHT rotamers have lower enthalpy and entropy than the HH rotamer (Table 4). Therefore, the higher entropy of the HH rotamer leads to the preference of this isomer over the MHT and mHT forms. The values of ΔH and ΔS for the MHT and mHT rotamers are more dispersed in the Bip than in the Me_4DAB complex. This greater dispersion can be easily understood by keeping in mind that in the former case the two HT rotamers are more different (the six-membered ring of Me_2Bzm is on the side of the N–CH_2– of the *cis* amine in one rotamer and on the side of the N–H of the *cis* amine in the other rotamer) than in the latter case (both rotamers have the six-membered ring of each Me_2Bzm on the side of a N–Me of the *cis* amine).

For both the Bip and Me_4DAB complexes, the MHT rotamer has higher enthalpy and entropy than the mHT rotamer, and this greater entropy makes the former rotamer favored. The opposite trend was observed in the related $Me_2DABPtG_2$ complexes (G = 9-ethylguanine, 3′-GMP, and 5′-GMP)[29] for which the major HT rotamer was always lower in enthalpy and entropy than the minor HT rotamer, and the lower enthalpy was responsible for the greater abundance of the former rotamer with respect to

the latter. This appears to be a major difference between Me_2Bzm and G derivatives and can be correlated to the presence, in corresponding positions of the base ring-systems, of a proton (H4) in one case and of an oxygen (O6) in the latter case.

Conclusions

Comparisons of analogous complexes containing two *cis* Me_2Bzm or two *cis* guanine ligands have clarified the factors influencing the properties of the guanine complexes. Electrostatic interactions between *cis* G's have been found to be the major driving force in base canting. The repulsion between O6 of *cis* G's is responsible for the "6-out" canting of at least one G in the HH rotamer. On the other hand, electrostatic attraction between the O6 of one G and the H8 of the *cis* G and base stacking are responsible for the preferential "6-in" canting of the two G's in the HT rotamer. The "6-out" canting of a base in the HH rotamer may be impeded by steric interaction between the six-membered ring of this base and a substituent on the *cis* amine. Similarly, the "6-in" canting of each base in the HT rotamer may be limited by steric interaction between the H8 of the base and a substituent on the *cis* amine.

The role of electrostatic interactions is greatly reduced in *cis*-$PtA_2(Me_2Bzm)_2$ complexes, as compared to the *cis*-PtA_2G_2 analogs, because the Me_2Bzm bases lack an oxygen substituent. Nevertheless, for both types of complexes the six-membered rings of the two bases are found on the most crowded side of the *cis* amine with respect to the coordination plane for the major HT rotamer. Also, for both types of complexes the major HT has the signal for the five-membered ring proton (H2 for Me_2Bzm and H8 for G) less shielded than the signal of that proton of the minor HT. As previously concluded for *cis*-PtA_2G_2 analogs, these findings are clear indications that for Me_2Bzm complexes also the major HT rotamer has more canted "6-in" bases than the minor HT rotamer and that such a greater canting is favored by smaller steric interactions between the H2 proton of each base and substituents on the *cis* amine. In the absence of major electrostatic interactions, the driving force for such a "6-in" canting of the two Me_2Bzm bases is likely to be base-stacking.

Thermodynamic parameters confirm the crucial role played by the H4 and O6 substituents (for Me_2Bzm and G derivatives, respectively) in determining the stability of different rotamers.

Experimental Section

Materials: 5,6-Dimethylbenzimidazole was purchased from Aldrich. (*R*,*S*,*S*,*R*)-BipPt$(NO_3)_2$, (*S*,*R*,*R*,*S*)-BipPt$(NO_3)_2$, *rac*-BipPt$(NO_3)_2$,[24] (*S*,*S*)-Me_4DABPt$(NO_3)_2$, (*R*,*R*)-Me_4DABPt$(NO_3)_2$, and *rac*-Me_4DABPt$(NO_3)_2$ were synthesized as described elsewhere.[23]

Preparation of $[Me_4DABPt(Me_2Bzm)_2]^{2+}$ Complexes: Stock solutions of (*R*,*S*,*S*,*R*)-BipPt$(NO_3)_2$, (*S*,*R*,*R*,*S*)-BipPt$(NO_3)_2$, (*S*,*S*)-Me_4DABPt$(NO_3)_2$, and (*R*,*R*)-Me_4DABPt$(NO_3)_2$ (4 mM) and of *rac*-BipPt$(NO_3)_2$ and *rac*-Me_4DABPt$(NO_3)_2$ (ca. 8 mM) were prepared in D_2O. NMR samples were prepared by adding 300 μL of complex solution into an NMR tube containing a suspension of 5,6-Me_2Bzm in 350 μL of H_2O (Me_2Bzm:Pt = 2.3). The pH was adjusted to 6 with 1% DNO_3. The reaction, monitored by ^1H NMR spectroscopy (23 °C), required several days (at, 55 °C) for completion.

NMR Spectroscopy: 1D NMR spectroscopic data were collected with Unity Varian 600 MHz and Inova 600 MHz instruments. A selective presaturation pulse was employed to suppress the HDO resonance, and the residual HDO peak was used as reference. FID's were accumulated for 64 scans.

2D experiments were performed in D_2O with a Unity Varian 600 MHz spectrometer. 2048 × 512 Matrices were collected at 5 °C for rotational nuclear Overhauser (ROESY) and $^1H/^1H$ nuclear Overhauser (NOESY) experiments (spectral window of ca. 6000 Hz in both dimensions), 2048 × 256 Matrices were collected at 25 °C for $^1H/^{13}C$ heteronuclear multiple-quantum coherence experiments (HMQC).

Circular Dichroism (CD) Spectroscopy: Solutions (ca. 0.04 mM) for CD experiments were prepared by diluting 30 μL of the NMR solution into 3 mL of H_2O. CD spectra were recorded at room temperature from 350 to 200 nm on a JASCO J-600 CD spectropolarimeter.

Thermodynamic Parameters: The equilibrium constants (K_{MHT} = [MHT]/[HH] and K_{mHT} = [mHT]/[HH]) were evaluated from the percentages of the different rotamers at different temperatures. The plots of $\ln K_{MHT}$ and $\ln K_{mHT}$ as a function of $1/T$ were linear within the experimental errors, and from their slopes and intercepts the values of ΔH and ΔS for the transformations were evaluated. The estimated thermodynamic parameters are listed in Table 4.

Supporting Information (see footnote on the first page of this article): Assignment of the Me5, Me6, and H7 signals of the Me_2Bzm ligand for $[rac\text{-BipPt}(Me_2Bzm)_2]^{2+}$ and $[rac\text{-}Me_4DABPt(Me_2Bzm)_2]^{2+}$. Equilibrium constants K_{MHT} and K_{mHT} at different temperatures and plots of the logarithm of the equilibrium constants as a function of $1/T$.

Acknowledgments

This work was supported by NIH Grant GM 29222 to LGM. We also acknowledge Dr. J. S. Saad, Prof. R. Cini, and members of COST D20 W.G. 001 and 003 for helpful discussions.

[1] J. Reedijk, *Chem. Commun.* **1996**, 801–806.
[2] M. J. Bloemink, J. Reedijk, in: *Metal Ions in Biological Systems*, vol. 32, **1996**, 641–685.
[3] S. E. Sherman, S. J. Lippard, *Chem. Rev.* **1987**, *87*, 1153–1181.
[4] T. P. Kline, L. G. Marzilli, D. Live, G. Zon, *J. Am. Chem. Soc.* **1989**, *111*, 7057–7068.
[5] C. S. Fouts, L. G. Marzilli, R. A. Byrd, M. F. Summers, G. Zon, K. Shinozuka, *Inorg. Chem.* **1988**, *27*, 366–376.
[6] M. Iwamoto, S. Mukundan Jr., L. G. Marzilli, *J. Am. Chem. Soc.* **1994**, *116*, 6238–6244.
[7] H. C. Wong, R. Coogan, F. P. Intini, G. Natile, L. G. Marzilli, *Inorg. Chem.* **1999**, *38*, 777–787.
[8] Y. Xu, G. Natile, F. P. Intini, L. G. Marzilli, *J. Am. Chem. Soc.* **1990**, *112*, 8177–8179.
[9] D. Kiser, F. P. Intini, Y. Xu, G. Natile, L. G. Marzilli, *Inorg. Chem.* **1994**, *33*, 4149–4158.
[10] S. O. Ano, F. P. Intini, G. Natile, L. G. Marzilli, *J. Am. Chem. Soc.* **1997**, *119*, 8570–8571.
[11] L. G. Marzilli, F. P. Intini, D. Kiser, H. C. Wong, S. O. Ano, P. A. Marzilli, G. Natile, *Inorg. Chem.* **1998**, *37*, 6898–6905.

[12] S. O. Ano, F. P. Intini, G. Natile, L. G. Marzilli, *Inorg. Chem.* **1999**, *38*, 2989–2999.
[13] S. T. C. Sullivan, A. Ciccarese, F. P. Fanizzi, L. G. Marzilli, *Inorg. Chem.* **2001**, *40*, 455–462.
[14] S. T. Sullivan, A. Ciccarese, F. P. Fanizzi, L. G. Marzilli, *Inorg. Chem.* **2000**, *39*, 836–842.
[15] R. E. Cramer, P. L. Dahlstrom, *J. Am. Chem. Soc.* **1979**, *101*, 3679–3681.
[16] J. Saad, T. Scarcia, G. Natile, L. G. Marzilli, *Inorg. Chem.* **2002**, *41*, 4923–4935.
[17] J. S. Saad, T. Scarcia, K. Shinozuka, G. Natile, L. G. Marzilli, *Inorg. Chem.* **2002**, *41*, 546–557.
[18] H. C. Wong, K. Shinozuka, G. Natile, L. G. Marzilli, *Inorg. Chim. Acta* **2000**, *297*, 36–46.
[19] M. Benedetti, J. S. Saad, L. G. Marzilli, G. Natile, *Dalton Trans.* **2003**, 872–879.
[20] J. D. Orbell, M. R. Taylor, S. L. Birch, S. E. Lawton, L. M. Vilkins, L. J. Keefe, *Inorg. Chim. Acta* **1988**, *152*, 125–134.
[21] M. Benedetti, G. Tamasi, R. Cini, G. Natile, *Chem. Eur. J.* **2003**, *9*, 6122–6132.
[22] E. Alessio, M. Calligaris, M. Iwamoto, L. G. Marzilli, *Inorg. Chem.* **1996**, *35*, 2538–2545.
[23] J. S. Saad, M. Benedetti, G. Natile, L. G. Marzilli, manuscript in preparation.
[24] S. O. Ano, F. P. Intini, G. Natile, L. G. Marzilli, *J. Am. Chem. Soc.* **1998**, *120*, 12017–12022.
[25] In previous related papers from our laboratories the expression "canted G base" was used to mean a G whose H8 experiences an upfield shifting effect caused by the ring-current anisotropy of the *cis* base (J. Kozelka, M. H. Fouchet, J. C. Chottard, *Eur. J. Biochem.* **1992**, *205*, 895–906). Conversely, the expression "uncanted base" was used to mean a G whose H8 is positioned away from the *cis* G and, therefore, is less shielded. In this paper the expression "canting" has been used to mean exclusively the sloping of a guanine plane on the coordination plane.
[26] The calculation has been performed starting from the X-ray structure of $Me_4DACHPtG_2$ ΔHT rotamer (ref.[21]) and rotating the two G's about the Pt–N7 bonds so as to have an HH conformer with guanine bases orthogonal to the coordination plane. Under these conditions the O6···O6 distance was found to be ca. 2.0 Å (sum of the van der Waals radii ca. 3.0 Å).
[27] E. Alessio, L. Hansen, M. Iwamoto, L. G. Marzilli, *J. Am. Chem. Soc.* **1996**, *118*, 7593–7600.
[28] The calculation has been performed starting from the X-ray structure of $Me_4DACHPtG_2$ ΔHT rotamer (ref.[21]) and rotating the two G's about the Pt–N7 bonds so as to reach a given canting angle. For each canting angle the O6···H8 distance between the two G's has been measured.
[29] G. Colonna, N. G. Di Masi, L. G. Marzilli, G. Natile, *Inorg. Chem.* **2003**, *42*, 997–1005.

Received: January 13, 2005
Published Online: June 2, 2005

